

## Collagen XVIII Deposition in the Basement Membrane Zone beneath the Newly Forming Epidermis during Wound Healing in Mice

Takahiro Maeba<sup>a</sup>, Tomoko Yonezawa<sup>a\*</sup>, Mitsuaki Ono<sup>a</sup>, Yasuko Tomono<sup>b</sup>,  
Ritva Heljasvaara<sup>c,d</sup>, Taina Pihlajaniemi<sup>e</sup>, Kiichi Inagawa<sup>e</sup>, and Toshitaka Oohashi<sup>a</sup>

<sup>a</sup>Department of Molecular Biology and Biochemistry, Okayama University Graduate School of Medicine,  
Dentistry and Pharmaceutical Science, Okayama 700-8558, Japan, <sup>b</sup>Shigei Medical Research Institute,

Okayama 701-0202, Japan, <sup>c</sup>Oulu Center for Cell-Matrix Research, Biocenter Oulu,

Faculty of Biochemistry and Molecular Medicine, University of Oulu, Oulu FIN-90014, Finland,

<sup>d</sup>Center for Cancer Biomarkers CCBIO, Department of Biomedicine, University of Bergen, Bergen N-5009, Norway,

<sup>e</sup>Department of Plastic and Reconstructive Surgery, Kawasaki Medical School, Kurashiki, Okayama 701-0192, Japan

The basement membrane (BM) is composed of various extracellular molecules and regulates tissue regeneration and maintenance. Here, we demonstrate that collagen XVIII was spatiotemporally expressed in the BM during skin wound healing in a mouse excisional wound-splinting model. Re-epithelialization was detected at days 3 and 6 post-wounding. The ultrastructure of epidermal BM was discontinuous at day 3, whereas on day 6 a continuous BM was observed in the region proximal to the wound edge. Immunohistochemistry demonstrated that collagen XVIII was deposited in the BM zone beneath newly forming epidermis in day 3 and 6 wounds. Laminin-332, known to be the earliest BM component appearing in wounds, was colocalized with collagen XVIII in the epidermal BM zone at days 3 and 6. The deposition of  $\alpha 1(\text{IV})$  collagen and nidogen-1 in the epidermal BM zone occurred later than that of collagen XVIII. We also observed the short isoform of collagen XVIII in the epidermal BM zone at day 3 post-wounding. Collectively, our results suggested that collagen XVIII plays a role in the formation of the dermal-epidermal junction during re-epithelialization, and that it is the short isoform that is involved in the early phase of re-epithelialization.

**Key words:** collagen XVIII, basement membrane, wound healing, re-epithelialization, skin

The skin covers the entire external surface of the body and maintains the body's homeostasis. The skin not only forms an effective barrier against various forms of environmental damage and microbial invasion, but also maintains moisture and biochemical metabolism. Following injury, skin wound healing is rapidly initiated and occurs efficiently in several phases: hemostasis, inflammation, granulation tissue formation, re-epithelialization, neovascularization, and remodeling [1, 2]. Re-epithelialization is an important step in

repairing damaged skin, and is accomplished by the migration, proliferation, and differentiation of keratinocytes. Keratinocytes migrate on the fibrinogen/fibrin-rich and fibronectin-rich provisional extracellular matrix (ECM), followed by a newly forming dermal-epidermal junction through the concerted action of epidermal and dermal cells [3, 4].

The basement membrane (BM) is a sheet-like ECM found beneath epithelial cells and surrounding blood vessels and muscle cells. The BM is composed of collagen IV, laminin, nidogen, perlecan and other glyco-

proteins. It provides mechanical support, separates tissue into different compartments, serves as a selective molecular sieve, and influences cell phenotypes, including cellular proliferation, migration, differentiation, and death [5,6].

Collagen IV comprises six  $\alpha$  chains, *i.e.*,  $\alpha 1$  (IV) to  $\alpha 6$  (IV), and three molecular forms have been identified:  $\alpha 1\alpha 2\alpha 1$  (IV),  $\alpha 3\alpha 4\alpha 5$  (IV) and  $\alpha 5\alpha 6\alpha 5$  (IV). The  $\alpha 1$  (IV),  $\alpha 2$  (IV),  $\alpha 5$  (IV) and  $\alpha 6$  (IV) chains are present in the epidermal BM [7,8]. Collagen IV molecules form mesh-like networks, providing a molecular scaffold for interactions between other BM components to form a mature BM. These scaffolds provide structural support for nearby cells [9-11]. Laminins are major components of the BM and form heterotrimeric molecules in a tissue-specific manner. For example, laminin-511 and laminin-521 are preferentially expressed in the epidermal BM. Laminin-332 is an essential component of the dermal-epidermal junction that acts as an anchoring filament; it is expressed immediately post-wound to promote keratinocyte adhesion and migration [4,12-14]. Mutations in the *LAMA3*, *LAMB3* and *LAMC2* genes cause junctional epidermolysis bullosa, which is characterized by skin fragility and mechanically induced blistering [15,16]. Both perlecan and nidogen bridge the scaffolds formed by laminin and collagen IV [17-19].

In addition to these major components, collagen XVIII, which is a heparan sulfate proteoglycan, is known to exist widely in various BMs. It is structurally characterized by a collagenous triple-helical domain with multiple interruptions flanked by an N-terminal thrombospondin domain and a C-terminal endostatin (ES) domain, and by glycosaminoglycan side chains. The gene encoding collagen XVIII is known to generate three distinct variants: the short, medium and long isoforms. Recent studies have demonstrated that these three isoforms differ in tissue distribution and functions (for review see [20]). Two alternative promoters drive the expression of the short transcript or the long transcript, and the latter is alternatively spliced to generate the medium isoform [21-24]. The three isoforms have N-terminal non-collagenous (NC) domains of different lengths, but their collagenous and C-terminal NC domains are identical. The C-terminal NC-1 domain includes ES, which has been found to have anti-angiogenic and anti-tumorigenic activities [25]. The short collagen XVIII isoform is the predominant form in epi-

thelial and endothelial BMs, and the longer isoforms are produced particularly in the liver and kidney glomeruli [26-28]. In humans, mutations in the *COL18A1* gene result in Knobloch syndrome, which is characterized by severe ocular abnormalities and occipital skull defects, and sometimes result in other manifestations such as renal abnormalities and hypertriglyceridemia [20]. Collagen XVIII-deficient (*Col18a1*<sup>-/-</sup>) mice display severe eye abnormalities like those reported in Knobloch patients [29-32]. The characterization of isoform-specific mutant mice lacking expression of the short isoform has revealed that the absence of the short isoform is sufficient to cause the eye defects found in Knobloch patients [33]. Mice lacking the medium and long isoforms display hypertriglyceridemia mediated by the impairment of adipocyte maturation and a decrease in the number of adipocytes [28].

In regard to the distribution of collagen XVIII in human skin, it has been demonstrated that the short and medium and/or long isoforms are present in the epidermal BM, and only the short isoform is present in the BMs surrounding blood vessels and muscle cells [27]. *In situ* hybridization further showed that collagen XVIII mRNA was expressed in keratinocytes of the epidermis in human adult and fetal skin [27]. However, the expression pattern and function of each isoform of collagen XVIII in skin wound healing are unknown.

Seppinen *et al.* reported that skin wound healing was delayed in ES-transgenic (tg) mice but accelerated in *Col18a1*<sup>-/-</sup> mice; however, there was no difference in the re-epithelialization rate at day 3 post-wound between the *Col18a1*<sup>-/-</sup> or ES-tg mice and the control mice [34]. The faster wound healing in the *Col18a1*<sup>-/-</sup> mice was attributed to an increased number of contracting myofibroblasts in the knockout wounds [34]. The vascularization rate of the granulation tissue was unaltered in ES-tg mice but was more rapid in the *Col18a1*<sup>-/-</sup> mice [34]. The presence of excess ES affected the structure and formation of epidermal and vascular BMs in skin wound healing [34].

Collagen XVIII exhibits a polarized orientation in BMs underlying the epidermis and retinal pigment epithelial cells, and in the kidney glomerular BM [24,26]. The binding activity of the C-terminal NC-1 domain to perlecan and other BM components appears to play a structural role. Interestingly, *Col18a1*<sup>-/-</sup> and ES-tg mice display widening of the lamina densa of the epidermal BM in electron microscopy [26,35-37]. The expression

of collagen XVIII and the binding of its C-terminal NC-1 domain to perlecan and other BM components thus appear to be important for the integrity of BMs.

The use of rodents to assess the processes of skin wound healing has frequently been criticized because of the rapid wound contraction. In the present study, we used the so-called splinting model of skin wound healing to evaluate the deposition of collagen XVIII and other ECM components in the epidermal BM. This model better mimics the wound healing in humans, as it has a proper excisional defect size to assess the re-epithelialization process and uses a silicone splint to minimize the rate of wound contraction [38]. We thus used this wound-splinting model to explore the role of collagen XVIII in the epidermal BM. Herein we describe the spatiotemporal expression of collagen XVIII isoforms in the dermal-epidermal junction in the splinting model, which may provide insights into the roles of this collagen in wound healing.

## Materials and Methods

**Animal experiments.** Eight-week-old C57BL/6J mice were purchased from CLEA Japan (Tokyo). All animal experiments were performed in accord with the approved protocols and guidelines of the Animal Research Committee at Okayama University (OKU-2015427 and -2017051). The wound model was established as described by Galiano *et al.* [38]. In brief, full-thickness defects, including those of panniculus muscle, were made using an 8-mm biopsy punch (Kai Industries, Seki, Gifu, Japan) in the dorsal skin of the mouse after hair removal under anesthesia with oxygen and 2% isoflurane inhalation (Pfizer, New York, NY, USA). A splint made from a 1-mm-thick silicone sheet was fixed to the skin using Aron Alpha<sup>®</sup> (Toagosei, Tokyo) and 5-0 nylon sutures, and the wounds were covered with IV3000 (Smith & Nephew, London, UK) as an occlusive dressing. Wound tissues were harvested at days 3, 6 and 9 post-wounding. Three mice were used for each time point of each experiment.

**Histological study.** Tissues were embedded in Tissue-Tek<sup>®</sup> O.C.T. compound (Sakura Finetek Japan, Tokyo) and snap-frozen in liquid nitrogen. Cryosections (8- $\mu$ m-thick) were fixed with 4% paraformaldehyde for 15 min and stained with hematoxylin and eosin (HE). For immunohistochemistry, cryosections (8- $\mu$ m-thick) were fixed in acetone for 20 min at room

temperature and were blocked in phosphate-buffered saline (PBS) with 1% bovine serum albumin (Sigma, St. Louis, MO, USA) for 3 h at room temperature. Before blocking, specimens for collagen IV staining were treated with 6 M urea in 0.1 M glycine (pH 3.5) for 10 min and incubated in 2 N HCl at 37°C for 10 min to expose the epitopes, as described previously [39].

The sections were incubated with the primary antibodies at 4°C overnight. After washing, the specimens were incubated with secondary antibodies for 40 min at room temperature, and nuclei were stained with Hoechst 33258 (Polysciences, Warrington, PA, USA). All images were taken with a BZ-700 microscope equipped with a BZ analyzer (Keyence, Osaka, Japan) and measured by ImageJ software (U.S. National Institutes of Health, Bethesda, MD, USA) for the analysis of re-epithelialized length, wound length, and immunopositive length in the sections of the central wound area. The re-epithelialized length was defined as the length of epithelial growth from the wound edge, and the wound length was defined as the length between the wound edges.

**Transmission electron microscopy (TEM).** Wound tissues harvested on days 3 and 6 were fixed with 2% glutaraldehyde and 2% paraformaldehyde in phosphate buffer at 4°C overnight. Specimens were postfixed with 2% osmium tetroxide in 0.1 M phosphate buffer for 1.5 h at 4°C. After dehydration with ethanol, the specimens were embedded in Spurr resin (Polysciences) and cut in ultrathin sections (LEICA EM UC7; Leica Mikrosysteme, Vienna, Austria). The ultrathin sections were stained with uranyl acetate and lead citrate and examined using a transmission electron microscope (H-7650; Hitachi, Tokyo) at the Central Research Laboratory, Okayama University Medical School.

**Antibodies.** A rat monoclonal antibody, CM186, against the NC1 domain of mouse collagen XVIII was used [40]. CM186 reacts with all three isoforms of mouse collagen XVIII. Other primary antibodies were used as follows: rat monoclonal antibody H11 against  $\alpha$ 1(IV) collagen [41-43], rat monoclonal antibody against perlecan (A7L6; Merck Millipore, Burlington, MA, USA), rabbit polyclonal antibody Q36.4 specific to the medium and long collagen XVIII isoforms (Medium/Long-18) [28], rabbit polyclonal antibody against laminin-332 (Immundiagnostik, Bensheim, Germany), rabbit polyclonal antibody against nidogen-1 kindly provided by Dr. T. Sasaki (Oita

University) and rabbit monoclonal antibody against cytokeratin 14 (abcam, Cambridge, UK). The following were used as secondary antibodies in the immunohistochemistry: Alexa Fluor 488 conjugated-donkey anti-rat IgG (Life Technologies, Carlsbad, CA, USA) and Alexa Fluor 594 conjugated-donkey anti-rabbit IgG (Life Technologies). A negative control was established by immunostaining with only the secondary antibodies (data not shown).

**Quantitative real-time PCR (RT-qPCR).** The wound samples were homogenized using a bead beater-type homogenizer ( $\mu$ T-01; Taitec, Saitama, Japan) with 3-mm stainless beads (Taitec). Following homogenization, total RNA was extracted and purified by QIAzol<sup>®</sup> Lysis Reagent and an RNeasy<sup>®</sup> Mini Kit (Qiagen, Hilden, Germany), and the cDNAs were synthesized with ReverTra Ace reverse transcriptase (Toyobo, Osaka, Japan). A real-time quantitative polymerase chain reaction (RT-qPCR) was performed with KAPA SYBR FAST qPCR Master Mix (Kapa Biosystems, Wilmington, MA, USA) and the StepOnePlus<sup>™</sup> Real-Time PCR system (Applied Biosystems, Waltham, MA, USA). The relative RNA levels were calculated by the  $2^{-\Delta\Delta C_t}$  method. Values were normalized to *Gapdh* expression.

The primer sequences were as follows: the short isoform of *Col18a1*, 5'-GGATGTGCTCACCAGTTTGG-3' and 5'-GTCATCGATTTGTGAGATCTTC-3'; the medium isoform of *Col18a1*, 5'-CCAGACTCCCAGAGAATGTTG-3' and 5'-CCGGACATGAAACAGCAGC-3'; the long isoform of *Col18a1*, 5'-AGGAGGACGGTACTGTGTG-3' and 5'-TGAGGGTCATCGATTTGTGA-3'; *Gapdh*, 5'-ACAGCAACTCCCCTTCC-3' and 5'-TCCACCACCCTGTTGCTGTA-3'.

**Statistical analysis.** The results are presented as the mean  $\pm$  standard deviation (SD). All statistical analyses were performed using Student's unpaired *t*-tests and the IBM<sup>®</sup> SPSS<sup>®</sup> statistics ver. 20 software (IBM, Armonk, NY, USA). *P*-values < 0.05 were considered significant.

## Results

**Wound morphology in full-thickness skin wound healing in mice.** To validate our skin wound healing model in mice, we observed the morphology of full-thickness wounds at days 3, 6 and 9 post-wounding. The length of the re-epithelialization region and the

wound length were determined in HE-stained sections. The sections from the central wound area were used for the analysis. Wounds gradually decreased in size and by day 9 were approximately 50% of the size of the day 0 wound (Fig. 1A, B). The re-epithelialization length increased gradually and reached > 50% of the wound at day 6 (Fig. 1A, C). At day 9, re-epithelialization was complete (Fig. 1A, C).

To examine the ultrastructure of epidermal BM in the wounds at days 3 and 6, we performed TEM. We found a discontinuous lamina densa in the wound area at day 3, specifically formed only beneath hemidesmosomes (Fig. 1D). By contrast, a continuous lamina densa, which was linked with the lamina densa in the unwounded region, was detected in the region proximal to the wound edge at day 6. In the region distal to the wound edge at day 6, a discontinuous lamina densa was detected, as observed on day 3. Hemidesmosomes were also observed along the entire epidermal basal layer on day 3 and 6, except at the leading edge of the epidermis in wound tissue (data not shown).

Most of the hemidesmosomes in the wound were of an immature form (Fig. 1D). In the region distal to the wound edge of the day 3 and day 6 wounds, fibrin matrix was frequently observed under the newly formed epidermis as an electron-dense fibril-like structure (Fig. 1D, distal). The ultrastructure of the dermal-epidermal junction under the newly formed epidermis displayed BM formation with a different level of maturation between day 3 and day 6 wounds. We therefore used day 3 and day 6 wound tissues to investigate the expression of BM proteins during re-epithelialization in skin wound healing.

### **Collagen XVIII deposited in the dermal-epidermal junction during re-epithelialization.**

We performed immunohistochemistry to examine the distribution of BM proteins during re-epithelialization using day 3 and day 6 wounds. Collagen XVIII was detected in epidermal and blood vessel BMs in unwounded skin (Fig. 2A, D: All-18). At days 3 and 6, the newly forming cytokeratin 14-immunopositive epidermis was detected in the wound (Fig. 2G, H). Collagen XVIII was deposited in the newly formed epidermal BM zone at days 3 and 6 (Fig. 2G, H). Laminin-332 was deposited and completely colocalized with collagen XVIII in the epidermal BM zone at days 3 and 6 (Fig. 2A-F).

We next used immunohistochemistry to compare the spatiotemporal expressions of both collagen XVIII and

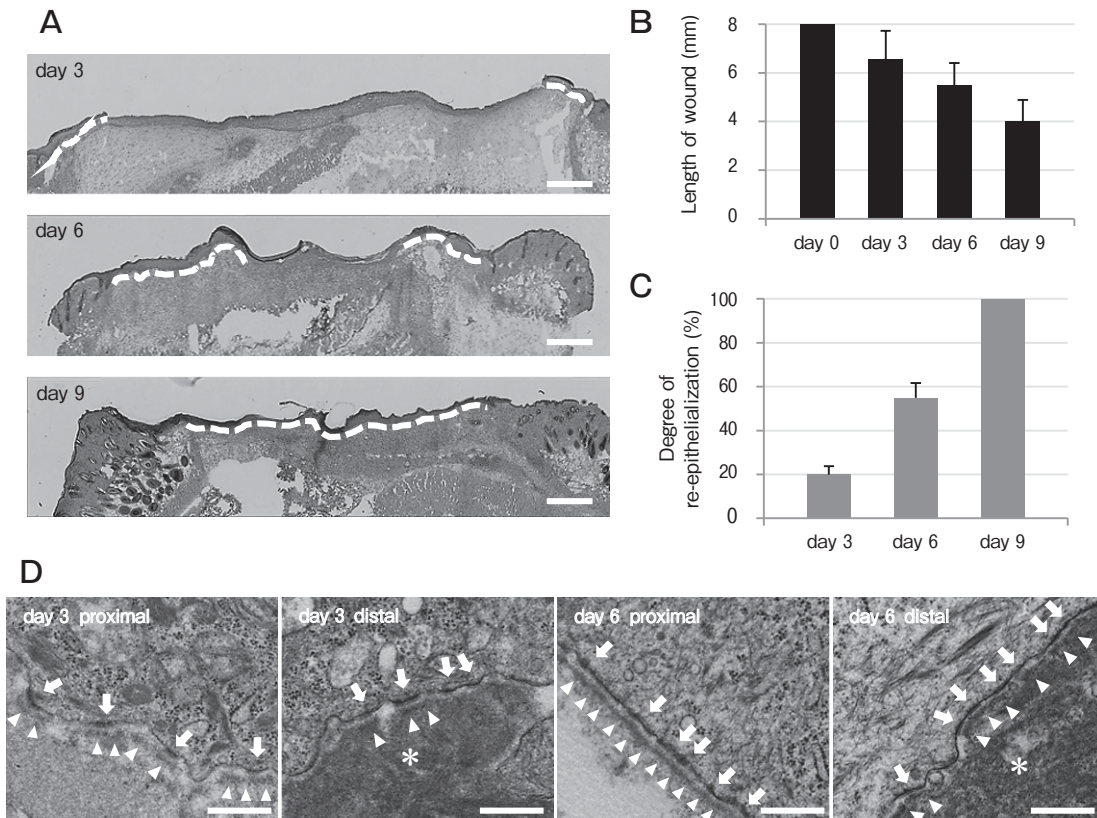


**Fig. 1** Histological analysis of full-thickness skin wounds in mice. **A**, Hematoxylin and eosin (HE) staining of sections from the central region of each wound at days 3, 6 and 9. Re-epithelialization was completed at day 9. *Dashed lines* indicate re-epithelialization in the wound area. Scale bars = 500  $\mu$ m; **B**, Wound length measured on HE-stained sections. The length of the day 0 wound was 8 mm. The wound length became gradually shorter. Values are mean  $\pm$  SD (all  $n = 3$ ); **C**, The relative length of re-epithelialization was measured on HE-stained sections. This length gradually increased, and the day 9 wounds were completely re-epithelialized. Values are mean  $\pm$  SD (all  $n = 3$ ); **D**, Ultrastructure of the dermal-epidermal junction of the proximal and distal regions to the wound edge at days 3 and 6. The lamina densa (*arrowheads*) was discontinuous in both the proximal and distal regions at day 3. By contrast, the lamina densa was discontinuous in the distal region but was restored in the region proximal to the wound edge at day 6. Fibrin (\*) was observed under the basal epidermis in the region distal to the wound edge. *Arrows* indicate hemidesmosomes. Scale bars = 5  $\mu$ m.

laminin-332 to those of collagen IV, nidogen-1 and perlecan, which are known typical components of the epidermal BM (Figs. 3, 4). We also determined the length of these proteins' immunopositive signals in the newly formed epidermal BM zone in the wound (Fig. 5). Because the lengths of the immunopositive signals of collagen XVIII and laminin-332 were identical in the wound during re-epithelialization, we assessed the distribution and length of collagen IV, nidogen-1, and perlecan by double immunostaining with either collagen XVIII or laminin-332.

Neither  $\alpha 1$  (IV) collagen nor nidogen-1 was detected in the newly formed epidermal BM zone at day 3 (Fig. 3A-F). At day 6,  $\alpha 1$  (IV) collagen and nidogen-1

were detected in the newly formed epidermal BM zone (Fig. 4A-F), but their lengths ( $76.78 \pm 23.93\%$  and  $74.13 \pm 22.01\%$ , respectively), although slightly shorter than that of laminin-332/collagen XVIII, were not significantly different ( $p = 0.384$  and  $0.268$ , respectively) ( $n = 3$ ) (Fig. 5). Perlecan was expressed in the newly formed BM zone at days 3 and 6 (with the respective lengths of  $76.60 \pm 18.02\%$  and  $91.59 \pm 6.49\%$ ); both of these lengths were slightly but not significantly shorter than that of laminin-332 (Fig. 3G-I, 4G-I;  $p = 0.374$  and  $0.832$ , respectively) ( $n = 3$ ) (Fig. 5).

**Distinct expression patterns depending on the collagen XVIII isoform in re-epithelialization.** The short, medium, and long isoforms of collagen XVIII

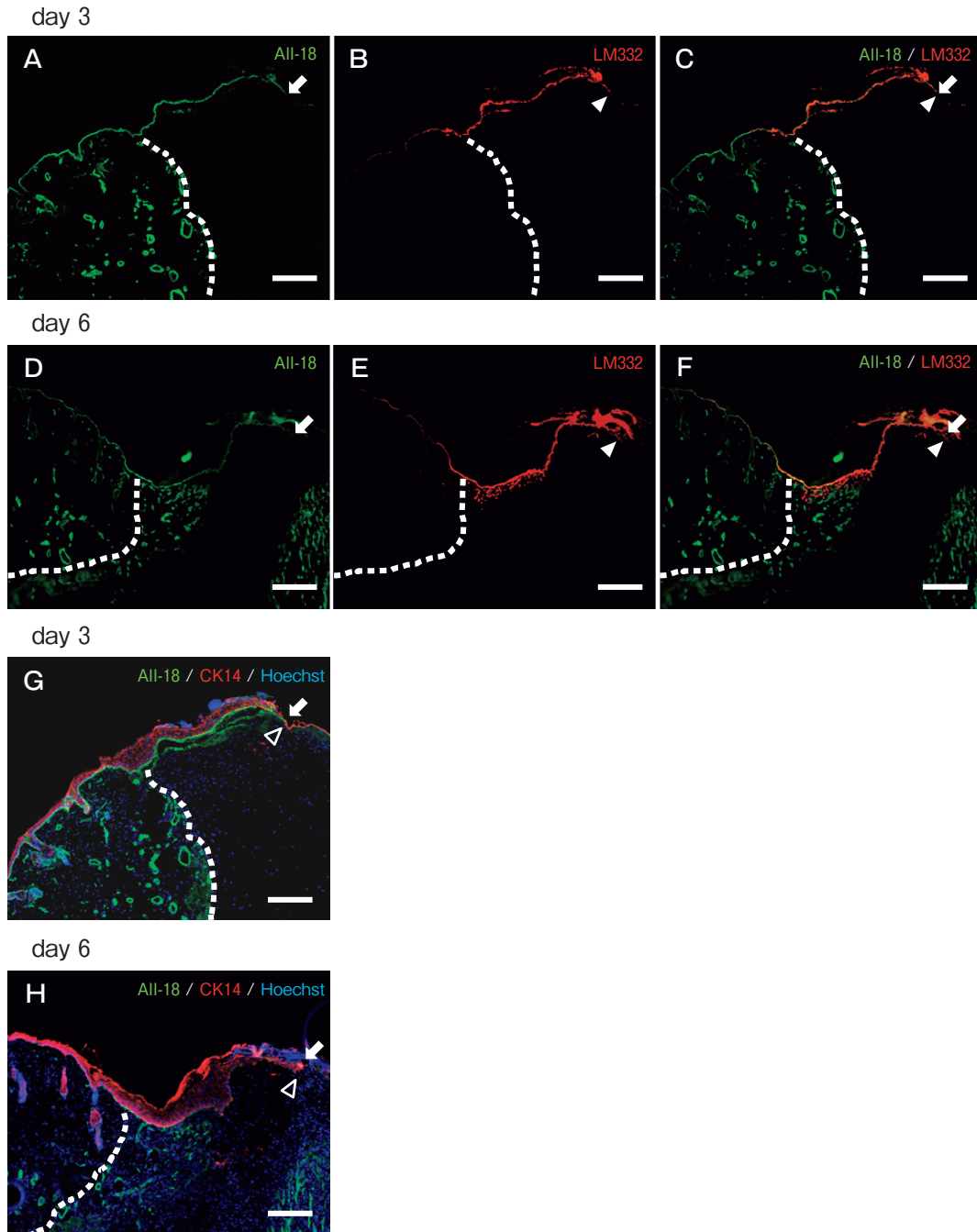


**Fig. 2** Collagen XVIII expression during re-epithelialization. Distribution of collagen XVIII (All-18: antibody that reacts with all collagen XVIII isoforms, *green*) (A, C, D, F, G, H), laminin-332 (LM332, *red*) (B, C, E, F) and cytokeratin 14 (CK14, *red*) (G, H) at days 3 (A–C, G) and 6 (D–F, H) post-wounding. Merged images are shown in C, F, G and H. Nuclei were counterstained with Hoechst 33258 (*blue*) (G, H). Collagen XVIII and laminin-332 were colocalized beneath cytokeratin 14-immunopositive epidermis in the wound at days 3 and 6. The edges of the immunopositive signal of collagen XVIII (*arrows*), laminin-332 (*arrowheads*) and cytokeratin 14 (*open arrowheads*) are indicated. *Dashed lines*: The wound border, to the right side of which is the wound region. Scale bars = 200  $\mu$ m.

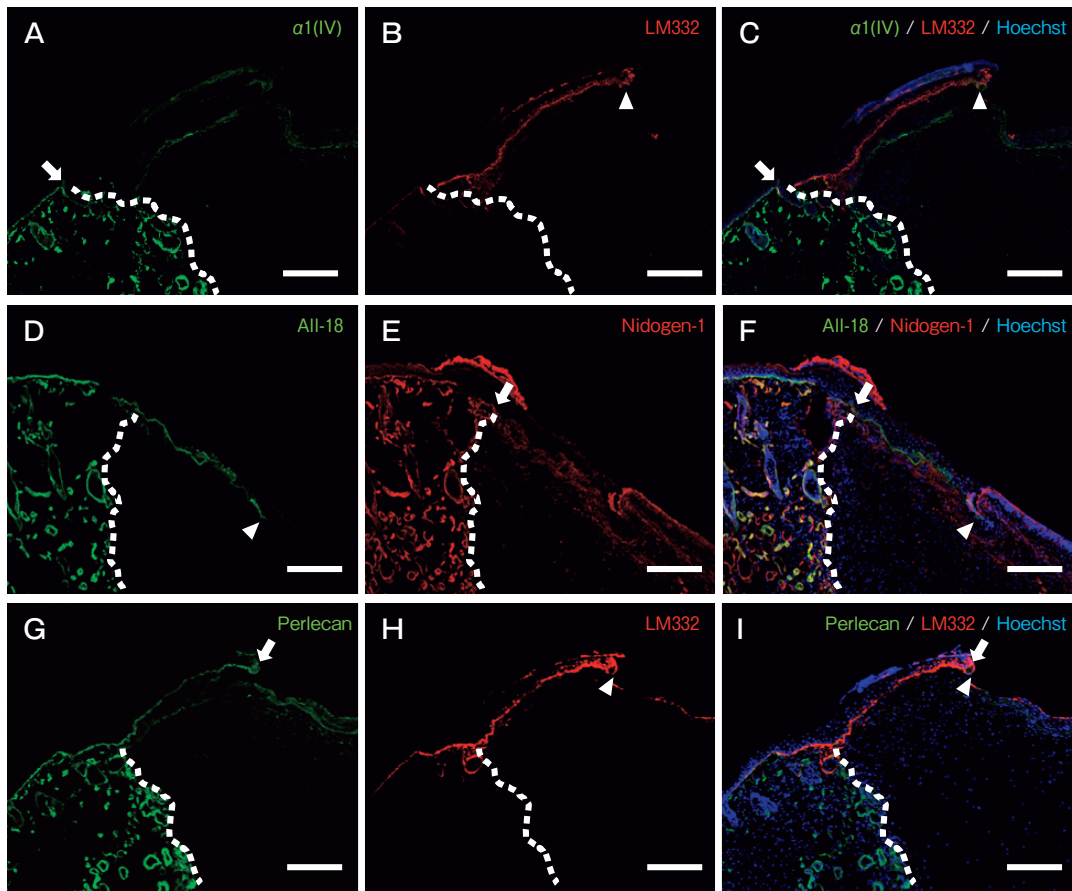


**Fig. 3** Comparison of the expression of epidermal BM proteins in a day 3 wound. Distributions of  $\alpha 1(IV)$  collagen ( $\alpha 1(IV)$ , *green*) (A, C), laminin-332 (LM332, *red*) (B, C, H, I), nidogen-1 (*red*) (E, F), perlecan (*green*) (G, I) and collagen XVIII (All-18: the antibody reacts with all collagen XVIII isoforms, *green*) (D, F) analyzed by immunohistochemistry. Merged images are shown in C, F and I. Nuclei were counterstained with Hoechst 33258 (*blue*). Collagen XVIII, laminin-332 and perlecan were detected in the newly formed dermal-epidermal junction at day 3, but  $\alpha 1(IV)$  collagen and nidogen-1 were not found at this time point. *Arrows*: The edge of the immunopositive signal of  $\alpha 1(IV)$  collagen (A, C), nidogen-1 (E, F) or perlecan (G, I). *Arrowheads*: the edge of the immunopositive signal of laminin-332 (B, C, H, I) or collagen XVIII (D, F). *Dashed lines*: The wound border, to the right side of which is the wound region. Scale bars = 200  $\mu$ m.

appear to have distinct functions in the human body [20]. We used immunohistochemistry to investigate which isoform(s) were associated with the promotion of epidermal BM formation after skin wounding. In unwounded skin, we detected an immunopositive signal using the antibody against the medium/long isoforms in the epidermal BM but not in blood-vessel BM (Fig. 6B, E). During wound healing, the deposition of the medium/long isoforms was not detected in the newly formed epidermal BM zone on day 3 (Fig. 6A-C).

By contrast, deposition of the medium/long isoforms was detected in the newly formed epidermal BM zone of day 6 wounds, but the length was shorter than

that of the antibody against all isoforms, including the short isoform of collagen XVIII (All-18) (Fig. 6D-F). The relative lengths of the medium/long isoforms at days 3 ( $16.21 \pm 12.74\%$ ) and 6 ( $53.93 \pm 8.05\%$ ) were significantly shorter than that of All-18 on both days ( $p = 0.032$  and  $0.023$ , respectively) ( $n = 3$ ) (Fig. 6A-G). Thus, our results demonstrated that the short isoform was the earliest isoform to appear in the newly forming epidermal BM zone during re-epithelialization.

We also compared the mRNA expression of each collagen XVIII isoform in day 3 wounds with that of day 0 wounds by real time RT-PCR. The relative mRNA expression level of the short isoform was

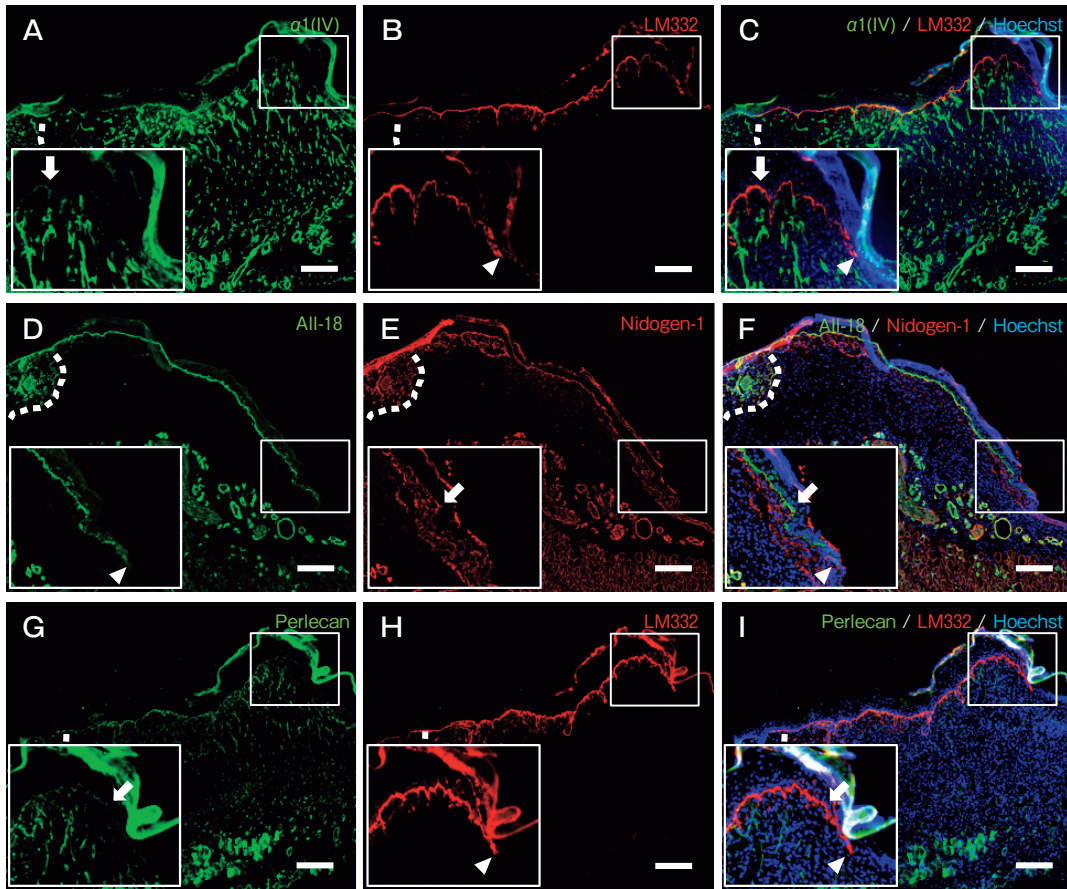


**Fig. 4** Comparison of the expressions of epidermal BM proteins in day 6 wounds. Distribution of  $\alpha 1(IV)$  collagen ( $\alpha 1(IV)$ , green) (A, C), laminin-332 (LM332, red) (B, C, H, I), nidogen-1 (red) (E, F), perlecan (green) (G, I) and collagen XVIII (All-18: the antibody reacts with all collagen XVIII isoforms, green) (D, F) analyzed by immunohistochemistry. Merged images are shown in C, F and I. Nuclei were counterstained with Hoechst 33258 (blue). Higher magnification of the area around the edge of the re-epithelialized epidermis in the boxes is shown in the respective insets.  $\alpha 1(IV)$  collagen, nidogen-1 and perlecan were detected in the newly formed dermal-epidermal junction. Arrows: The edge of the immunopositive signal of  $\alpha 1(IV)$  collagen (A, C), nidogen-1 (E, F) or perlecan (G, I). Arrowheads: The edge of the immunopositive signal of laminin-332 (B, C, H, I) or collagen XVIII (D, F). Dashed lines indicate the wound border, to the right side of which is the wound region. Scale bars = 200  $\mu$ m.

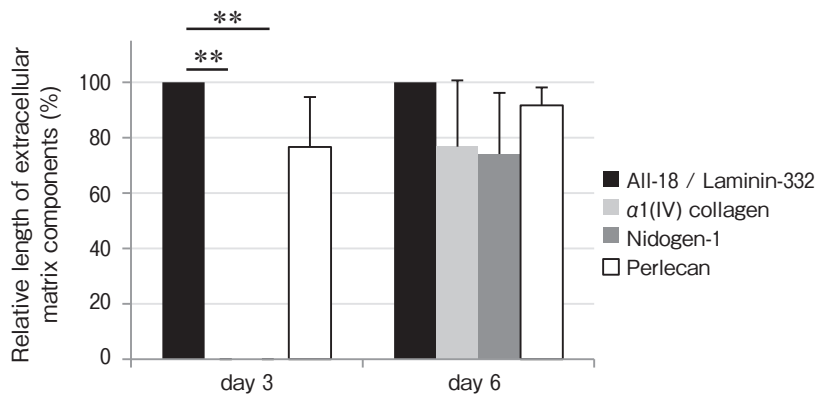


**Fig. 5** Differential expression of BM proteins in the dermal-epidermal junction post-wounding. The relative length of the immunopositive signal in the dermal-epidermal junction in day 3 and day 6 wounds is indicated. Values are mean  $\pm$  SD (all n = 3). \*\*  $p < 0.001$ .

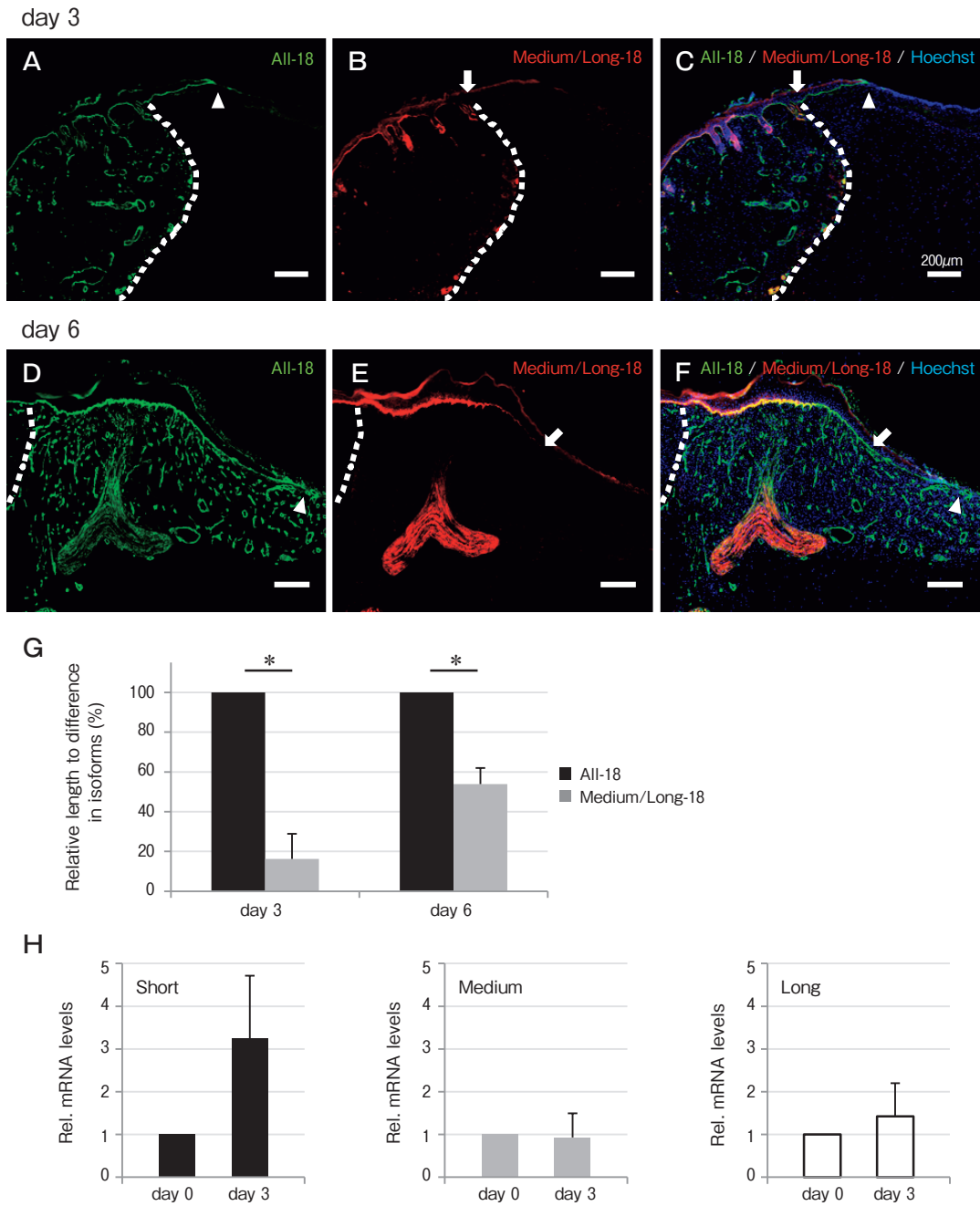


**Fig. 6** Distinct expression patterns of the different collagen XVIII isoforms during re-epithelialization. The distributions of collagen XVIII (All-18: the antibody reacts with all collagen XVIII isoforms, *green*) (**A, D**) and the medium/long isoforms of collagen XVIII (Medium/Long-18, *red*) (**B, E**) were analyzed by immunohistochemistry in day 3 (**A–C**) and 6 (**D–F**) wounds. Sections were double-immunostained, and the merged images are shown in **C** and **F**. Nuclei were counterstained with Hoechst 33258 (*blue*). *Arrows*: The edge of the immunopositive signal of the medium/long isoforms. *Arrowheads*: The edge of the immunopositive signal of collagen XVIII (All-18). *Dashed lines*: The wound border, to the right side of which is the wound region. Scale bars = 200 μm. **G**, The relative length of the immunopositive signal in the dermal-epidermal junction in the wound. Values are mean ± SD (all n = 3). \*p < 0.05; **H**, The mRNA expressions of the short, medium, and long isoforms in day 0 and day 3 wounds were analyzed by real-time RT-PCR. The most increased isoform in day 3 wounds was the short form. There were no significant differences in the mRNA expression of all of the isoforms between day 0 and day 3 wounds. Values are mean ± SD (all n = 3).

increased at day 3 to  $3.25 \pm 1.46$  (Fig. 6H), but this was not significantly greater than the value at day 0 ( $p=0.095$ ). Regarding the limited increase of the relative mRNA expression of the medium and long isoforms in day 3 wounds to  $0.93 \pm 0.56$  and  $1.43 \pm 0.77$ , respectively, these values were not significantly different from the day 0 wound values ( $p=0.872$  and  $0.480$ , respectively) ( $n=3$ ) (Fig. 6H).

## Discussion

Collagen XVIII is a component of epidermal and blood-vessel BMs in skin. In the present study, we investigated the collagen XVIII expression in skin wound healing in mice. The results demonstrated that collagen XVIII was deposited in the BM zone under the newly forming epidermis during re-epithelialization. Collagen XVIII may participate as one of the earliest BM molecules in the formation of the dermal-epidermal junction in skin wound healing.

Time-dependent expression patterns of several ECM components and related molecules (including integrin) have been observed during BM formation in skin equivalents by co-cultured keratinocytes and fibroblasts [44-47] and during skin wound healing *in vivo* [48, 49]. Laminin-332 is known to be expressed in the wound area prior to the other components of the BM, including collagen IV, perlecan and nidogen [12, 13, 45-50]. We noted that collagen XVIII was deposited in the epidermal BM zone at the same rate as migrating keratinocytes in the early wound healing phase, and the collagen XVIII expression spatiotemporally corresponded to that of laminin-332 (Fig. 2). Our findings also showed that the short collagen XVIII isoform was the earliest form deposited beneath the newly forming epidermis, and that the medium/ long isoforms were deposited later (Fig. 6A-G). The short isoform mRNA expression tended to be increased at day 3 post-wounding, but the medium and long isoform mRNA expressions were both minimally changed (Fig. 6H).

Interestingly, our TEM observations indicated that the lamina densa was discontinuously formed beneath the immature hemidesmosomes in day 3 wounds, and then became continuous and appeared normal in the region proximal to the wound edge at day 6 (Fig. 1). The observed sequential ultrastructural changes of the BM agreed with those seen in a cell-culture model of epidermal cells on a collagen gel [51]. Collagen IV is

known to be a major component of the lamina densa [18]. The results of our immunohistochemistry examinations showed that the collagen IV and nidogen-1 deposition in the BM zone were substantially delayed compared to those of laminin-332 and collagen XVIII (Figs. 3-5). It is likely that the appearance of a continuous lamina densa, namely a mature BM, corresponds to the depositions of collagen IV and nidogen-1 that we observed in the BM zone. Taken together, our findings indicate that (1) collagen XVIII was deposited in the BM zone identically to laminin-332 before the formation of a mature BM during re-epithelialization, and (2) the short isoform was most closely associated with the early events of re-epithelialization.

Perlecan, characterized as the most common heparan sulfate proteoglycan of BMs, was deposited in the epidermal BM zone earlier than collagen IV and nidogen-1 (Figs. 3-5). Heparan sulfate chains are associated with the multifunction ability of perlecan to bind various ECM molecules, cytokines and growth factors. Glycosaminoglycan side chains of collagen XVIII can mediate binding to BMs and form a growth-factor gradient [20, 52, 53]. Collagen XVIII and perlecan may collaborate by supplying glycosaminoglycan chains prior to the formation of a BM scaffold of collagen IV in re-epithelialization.

The formation of the dermal-epidermal junction is critical for repairing damaged skin. Because of the abnormality of the BM ultrastructure in several tissues of *Col18a1*<sup>-/-</sup> and ES-tg mice, collagen XVIII is thought to be important for the integrity of BMs. The binding activity of the NC-1 domain of collagen XVIII with other ECM components and integrins as receptors could be associated with the structural function [20, 36]. During re-epithelialization, the leading edge of the epidermis migrates over the fibrinogen/fibrin-rich and fibronectin-rich provisional matrix [4]. The interaction between collagen XVIII and fibrinogen has been established [54], and it was demonstrated that the fibrin deposition in injured liver was altered in *Col18a1*<sup>-/-</sup> mice [55]. The deposition of collagen XVIII under the migrating epidermis may promote the interaction between the epidermis and provisional matrix in the wound.

The C-terminal ES domain of the short isoform is normally directed at the plasma membrane whereas the N-terminus is oriented toward the fibrillary matrix in BMs in several tissues, including epidermal BM

[20,29,35]. The short and medium/long collagen XVIII isoforms are expressed in the glomerular basement membrane (GBM), which is present between endothelial cells and podocytes, and the C-terminal regions of all isoforms are embedded in the GBM [26]. The polarized presence of collagen XVIII in the BM is believed to be important in maintaining BM integrity and for its physiological functions. Our present results demonstrated that the short and medium/long isoforms are present in the epidermal BM during wound healing (Fig. 6). However, the isoform-specific functions and orientation in epidermal BM have not yet been identified. The dynamic construction of basement membranes depending on the phase and condition of skin wound healing is considered to be crucial for repairing damaged skin. Our results suggest that collagen XVIII plays a role in the formation of the dermal-epidermal junction during re-epithelialization.

**Acknowledgments.** We thank Drs. Yoshikazu Sado (Okayama Univ., Japan) and Takako Sasaki (Oita Univ., Japan) for providing antibodies; Ms. Masumi Furutani and Moemi Tsukano (Central Research Laboratory, Okayama University Medical School) for technical assistance with TEM; and Dr. Ryusuke Momota for his critical reading of the manuscript and insightful comments. This study was supported by a JSPS KAKENHI grant, no. JP17K11540.

## References

- Martin P: Wound healing—aiming for perfect skin regeneration. *Science* (1997) 276: 75–81.
- Gurtner GC, Werner S, Barrandon Y and Longaker MT: Wound repair and regeneration. *Nature* (2008) 453: 314–321.
- Barker TH and Engler AJ: The provisional matrix: setting the stage for tissue repair outcomes. *Matrix Biol* (2017) 60–61: 1–4.
- Rousselle P, Montmasson M and Garnier C: Extracellular matrix contribution to skin wound re-epithelialization. *Matrix Biol* (2018) in press.
- Pozzi A, Yurchenco PD and Iozzo RV: The nature and biology of basement membranes. *Matrix Biol* (2017) 57–58: 1–11.
- Yurchenco PD and Ruben GC: Basement membrane structure in situ: evidence for lateral associations in the type IV collagen network. *J Cell Biol* (1987) 105: 2559–2568.
- Saito K, Naito I, Seki T, Oohashi T, Kimura E, Momota R, Kishiro Y, Sado Y, Yoshioka H and Ninomiya Y: Differential expression of mouse alpha5(IV) and alpha6(IV) collagen genes in epithelial basement membranes. *J Biochem* (2000) 128: 427–434.
- Sado Y, Kagawa M, Naito I, Ueki Y, Seki T, Momota R, Oohashi T and Ninomiya Y: Organization and expression of basement membrane collagen IV genes and their roles in human disorders. *J Biochem* (1998) 123: 767–776.
- Brown KL, Cummings CF, Vanacore RM and Hudson BG: Building collagen IV smart scaffolds on the outside of cells. *Protein Sci* (2017) 26: 2151–2161.
- Khoshnoodi J, Pedchenko V and Hudson BG: Mammalian collagen IV. *Microsc Res Tech* (2008) 71: 357–370.
- Pöschl E, Schlötzer-Schrehardt U, Brachvogel B, Saito K, Ninomiya Y and Mayer U: Collagen IV is essential for basement membrane stability but dispensable for initiation of its assembly during early development. *Development* (2004) 131: 1619–1628.
- Nguyen BP, Ryan MC, Gil SG and Carter WG: Deposition of laminin 5 in epidermal wounds regulates integrin signaling and adhesion. *Curr Opin Cell Biol* (2000) 12: 554–562.
- Kurpakus MA, Stock EL and Jones JC: Analysis of wound healing in an in vitro model: early appearance of laminin and a 125 x 10(3) Mr polypeptide during adhesion complex formation. *J Cell Sci* (1990) 96 (Pt4): 651–660.
- Kainulainen T, Hakkinen L, Hamidi S, Larjava K, Kallioinen M, Peltonen J, Salo T, Larjava H and Oikarinen A: Laminin-5 expression is independent of the injury and the microenvironment during reepithelialization of wounds. *J Histochem Cytochem* (1998) 46: 353–360.
- Kiritisi D, Has C and Bruckner-Tuderman L: Laminin 332 in junctional epidermolysis bullosa. *Cell Adh Migr* (2013) 7: 135–141.
- Iozzo RV and Gubbiotti MA: Extracellular matrix: The driving force of mammalian diseases. *Matrix Biol* (2018) 71–72: 1–9.
- Hohenester E and Yurchenco PD: Laminins in basement membrane assembly. *Cell Adh Migr* (2013) 7: 56–63.
- Breitkreutz D, Koxholt I, Thiemann K and Nischt R: Skin basement membrane: the foundation of epidermal integrity—BM functions and diverse roles of bridging molecules nidogen and perlecan. *Biomed Res Int* (2013) 2013: 179784.
- Baranowsky A, Mokkaapati S, Bechtel M, Krügel J, Miosge N, Wickenhauser C, Smyth N and Nischt R: Impaired wound healing in mice lacking the basement membrane protein nidogen 1. *Matrix Biol* (2010) 29: 15–21.
- Heljasvaara R, Aikio M, Ruotsalainen H and Pihlajaniemi T: Collagen XVIII in tissue homeostasis and dysregulation - Lessons learned from model organisms and human patients. *Matrix Biol* (2017) 57–58: 55–75.
- Muragaki Y, Timmons S, Griffith CM, Oh SP, Fadel B, Quertermous T and Olsen BR: Mouse Col18a1 is expressed in a tissue-specific manner as three alternative variants and is localized in basement membrane zones. *Proc Natl Acad Sci U S A* (1995) 92: 8763–8767.
- Rehn M and Pihlajaniemi T: Identification of three N-terminal ends of type XVIII collagen chains and tissue-specific differences in the expression of the corresponding transcripts. The longest form contains a novel motif homologous to rat and *Drosophila* frizzled proteins. *J Biol Chem* (1995) 270: 4705–4711.
- Rehn M, Hintikka E and Pihlajaniemi T: Characterization of the mouse gene for the alpha 1 chain of type XVIII collagen (Col18a1) reveals that the three variant N-terminal polypeptide forms are transcribed from two widely separated promoters. *Genomics* (1996) 32: 436–446.
- Elamaa H, Snellman A, Rehn M, Autio-Harmainen H and Pihlajaniemi T: Characterization of the human type XVIII collagen gene and proteolytic processing and tissue location of the variant containing a frizzled motif. *Matrix Biol* (2003) 22: 427–442.
- O'Reilly MS, Boehm T, Shing Y, Fukai N, Vasios G, Lane WS, Flynn E, Birkhead JR, Olsen BR and Folkman J: Endostatin: an endogenous inhibitor of angiogenesis and tumor growth. *Cell* (1997) 88: 277–285.
- Kinnunen AI, Sormunen R, Elamaa H, Seppinen L, Miller RT, Ninomiya Y, Janmey PA and Pihlajaniemi T: Lack of collagen XVIII long isoforms affects kidney podocytes, whereas the short form is needed in the proximal tubular basement membrane. *J Biol*

- Chem (2011) 286: 7755–7764.
27. Saarela J, Rehn M, Oikarinen A, Autio-Harmainen H and Pihlajaniemi T: The short and long forms of type XVIII collagen show clear tissue specificities in their expression and location in basement membrane zones in humans. *Am J Pathol* (1998) 153: 611–626.
  28. Aikio M, Elamaa H, Vicente D, Izzi V, Kaur I, Seppinen L, Speedy HE, Kaminska D, Kuusisto S, Sormunen R, Heljasvaara R, Jones EL, Muilu M, Jauhainen M, Pihlajamäki J, Savolainen MJ, Shoulders CC and Pihlajaniemi T: Specific collagen XVIII isoforms promote adipose tissue accrual via mechanisms determining adipocyte number and affect fat deposition. *Proc Natl Acad Sci U S A* (2014) 111: E3043–E3052.
  29. Fukai N, Eklund L, Marneros AG, Oh SP, Keene DR, Tamarkin L, Niemelä M, Ilves M, Li E, Pihlajaniemi T and Olsen BR: Lack of collagen XVIII/endostatin results in eye abnormalities. *EMBO J* (2002) 21: 1535–1544.
  30. Utrianen A, Sormunen R, Kettunen M, Carvalhaes LS, Sajanti E, Eklund L, Kauppinen R, Kitten GT and Pihlajaniemi T: Structurally altered basement membranes and hydrocephalus in a type XVIII collagen deficient mouse line. *Hum Mol Genet* (2004) 13: 2089–2099.
  31. Ylikärppä R, Eklund L, Sormunen R, Kontiola AI, Utrianen A, Määttä M, Fukai N, Olsen BR and Pihlajaniemi T: Lack of type XVIII collagen results in anterior ocular defects. *FASEB J* (2003) 17: 2257–2259.
  32. Marneros AG and Olsen BR: Age-dependent iris abnormalities in collagen XVIII/endostatin deficient mice with similarities to human pigment dispersion syndrome. *Invest Ophthalmol Vis Sci* (2003) 44: 2367–2372.
  33. Aikio M, Hurskainen M, Brideau G, Hägg P, Sormunen R, Heljasvaara R, Gould DB and Pihlajaniemi T: Collagen XVIII short isoform is critical for retinal vascularization, and overexpression of the Tsp-1 domain affects eye growth and cataract formation. *Invest Ophthalmol Vis Sci* (2013) 54: 7450–7462.
  34. Seppinen L, Sormunen R, Soini Y, Elamaa H, Heljasvaara R and Pihlajaniemi T: Lack of collagen XVIII accelerates cutaneous wound healing, while overexpression of its endostatin domain leads to delayed healing. *Matrix Biol* (2008) 27: 535–546.
  35. Marneros AG, Keene DR, Hansen U, Fukai N, Moulton K, Goletz PL, Moiseyev G, Pawlyk BS, Halfter W, Dong S, Shibata M, Li T, Crouch RK, Bruckner P and Olsen BR: Collagen XVIII/endostatin is essential for vision and retinal pigment epithelial function. *EMBO J* (2004) 23: 89–99.
  36. Sasaki T, Fukai N, Mann K, Göhring W, Olsen BR and Timpl R: Structure, function and tissue forms of the C-terminal globular domain of collagen XVIII containing the angiogenesis inhibitor endostatin. *EMBO J* (1998) 17: 4249–4256.
  37. Elamaa H, Sormunen R, Rehn M, Soininen R and Pihlajaniemi T: Endostatin overexpression specifically in the lens and skin leads to cataract and ultrastructural alterations in basement membranes. *Am J Pathol* (2005) 166: 221–229.
  38. Galiano RD, Michaels J, Dobryansky M, Levine JP and Gurtner GC: Quantitative and reproducible murine model of excisional wound healing. *Wound Repair Regen* (2004) 12: 485–492.
  39. Yonezawa T, Ohtsuka A, Yoshitaka T, Hirano S, Nomoto H, Yamamoto K and Ninomiya Y: Limitrin, a novel immunoglobulin superfamily protein localized to glia limitans formed by astrocyte endfeet. *Glia* (2003) 44: 190–204.
  40. Tomono Y, Naito I, Ando K, Yonezawa T, Sado Y, Hirakawa S, Arata J, Okigaki T and Ninomiya Y: Epitope-defined monoclonal antibodies against multiplexin collagens demonstrate that type XV and XVIII collagens are expressed in specialized basement membranes. *Cell Struct Funct* (2002) 27: 9–20.
  41. Ninomiya Y, Kagawa M, Iyama K, Naito I, Kishiro Y, Seyer JM, Sugimoto M, Oohashi T and Sado Y: Differential expression of two basement membrane collagen genes, COL4A6 and COL4A5, demonstrated by immunofluorescence staining using peptide-specific monoclonal antibodies. *J Cell Biol* (1995) 130: 1219–1229.
  42. Hasegawa H, Naito I, Nakano K, Momota R, Nishida K, Taguchi T, Sado Y, Ninomiya Y and Ohtsuka A: The distributions of type IV collagen alpha chains in basement membranes of human epidermis and skin appendages. *Arch Histol Cytol* (2007) 70: 255–265.
  43. Saito K, Yonezawa T, Minaguchi J, Kurosaki M, Suetsugu S, Nakajima A, Nomoto H, Morizane Y, Sado Y, Sugimoto M, Kusachi S and Ninomiya Y: Distribution of  $\alpha$ (IV) collagen chains in the ocular anterior segments of adult mice. *Connect Tissue Res* (2011) 52: 147–156.
  44. Safferling K, Sütterlin T, Westphal K, Ernst C, Breuhahn K, James M, Jäger D, Halama N and Grabe N: Wound healing revised: a novel reepithelialization mechanism revealed by in vitro and in silico models. *J Cell Biol* (2013) 203: 691–709.
  45. Smola H, Stark HJ, Thiekötter G, Mirancea N, Krieg T and Fusenig NE: Dynamics of basement membrane formation by keratinocyte-fibroblast interactions in organotypic skin culture. *Exp Cell Res* (1998) 239: 399–410.
  46. Yamazoe K, Miyamoto S, Hikosaka Y, Kitagawa K, Watanabe K, Sakai H and Kudo T: Three-dimensional culture of keratinocytes and the formation of basement membrane for canine footpad substitute. *J Vet Med Sci* (2007) 69: 611–617.
  47. Laplante AF, Germain L, Auger FA and Moulin V: Mechanisms of wound reepithelialization: hints from a tissue-engineered reconstructed skin to long-standing questions. *FASEB J* (2001) 15: 2377–2389.
  48. Larjava H, Salo T, Haapasalmi K, Kramer RH and Heino J: Expression of integrins and basement membrane components by wound keratinocytes. *J Clin Invest* (1993) 92: 1425–1435.
  49. Betz P, Nerlich A, Wilske J, Tübel J, Wiest I, Penning R and Eisenmenger W: The time-dependent rearrangement of the epithelial basement membrane in human skin wounds—immunohistochemical localization of collagen IV and VII. *Int J Legal Med* (1992) 105: 93–97.
  50. Botta A, Delteil F, Mettouchi A, Vieira A, Estrach S, Négroni L, Stefani C, Lemichez E, Meneguzzi G and Gagnoux-Palacios L: Confluence switch signaling regulates ECM composition and the plasmin proteolytic cascade in keratinocytes. *J Cell Sci* (2012) 125: 4241–4252.
  51. Hirone T and Taniguchi S: Basal lamina formation by epidermal cells in cell culture. *Curr Probl Dermatol* (1980) 10: 159–169.
  52. Dong S, Cole GJ and Halfter W: Expression of collagen XVIII and localization of its glycosaminoglycan attachment sites. *J Biol Chem* (2003) 278: 1700–1707.
  53. Momota R, Naito I, Ninomiya Y and Ohtsuka A: Drosophila type XV/XVIII collagen, Mp, is involved in Wingless distribution. *Matrix Biol* (2011) 30: 258–266.
  54. Tang H, Fu Y, Lei Q, Han Q, Ploplis VA, Castellino FJ, Li L and Luo Y: Fibrinogen facilitates the anti-tumor effect of nonnative endostatin. *Biochem Biophys Res Commun* (2009) 380: 249–253.
  55. Duncan MB, Yang C, Tanjore H, Boyle PM, Keskin D, Sugimoto H, Zeisberg M, Olsen BR and Kalluri R: Type XVIII collagen is essential for survival during acute liver injury in mice. *Dis Model Mech* (2013) 6: 942–951.